

Supporting information

Surfactant decorated hydrotalcite-supported polyoxometalates for aerobic oxidation of 5-hydroxymethylfurfural and monosaccharides

Ping Cao, Ying Li, Yiming Li, Xueyan Zhang, Xiaohong Wang*^a and Zijiang Jiang*^b

^a Key Lab of Polyoxometalate Science of Ministry of Education, Faculty of Chemistry, Northeast Normal University, Changchun 130024, PR China. Fax: 0086-431-85099759; Tel.: 0086-431-

88930042; E-mail address: wangxh665@nenu.edu.cn.

^b Changchun Institute of Applied Chemistry, Chinese Academy of Sciences, National Analytical Research Center of Electrochemistry and Spectroscopy, Changchun 130024, PR China. E-mail address: zjjiang@ciac.ac.cn.

S1. Materials

S2. Physical measurements

S3. Aerobic oxidation of 5-HMF

S4. Aerobic oxidation of fructose or glucose

S5. Determination of the acidic and basic properties

Fig. S1 IR spectra of Mg₄Al-LDH (a), Mg₄Al-COOH (b), Mg₄Al-NH₂ (c), HPMoV@Mg₁Al-Surf (23) (d), HPMoV@Mg₂Al-Surf (23) (e), HPMoV@Mg₃Al-Surf (23) (f), HPMoV@Mg₄Al-Surf (23) (g), and HPMoV (h)

Fig. S2 IR spectra of HPMoV@Mg₄Al-Surf with different loading amount: Mg₄Al-LDH (a), HPMoV@Mg₄Al-Surf (5) (b), HPMoV@Mg₄Al-Surf (12) (c), HPMoV@Mg₄Al-Surf (17) (d), HPMoV@Mg₄Al-Surf (23) (e), HPMoV@Mg₄Al-Surf (28) (f), and HPMoV (g)

Fig. S3 DR-UV-vis spectra of the HPMoV@Mg₄Al-Surf (5-28)

Fig. S4 Water contact angle of Mg₄Al-LDH (a), Mg₄Al-NH₂ (b), Mg₄Al-Surf (c) and HPMoV@Mg₄Al-Surf (23) (d)

Fig. S5 XRD patterns of Mg₄Al-LDH, Mg₄Al-COOH, Mg₄Al-NH₂, HPMoV@Mg_nAl-Surf (23) (n = 1, 2, 3, 4) and HPMoV

Fig. S6 XRD patterns of Mg₄Al-LDH, HPMoV@Mg₄Al-Surf (5-28) and HPMoV

Fig. S7 Nitrogen adsorption-desorption isotherms (a) and pore size distribution profiles according to BJH desorption dV/dD pore volume (b) of Mg₄Al-LDH and HPMoV@Mg₄Al-Surf (5-28)

Fig. S8 The Energy-dispersive spectroscopy (EDX) mapping of HPMoV@Mg₄Al-Surf (23)

Fig. S9 The EDAX of Mg₄Al-LDH (a) and HPMoV@Mg₄Al-Surf (5-28) (b-f)

Fig. S10 IR spectra of pyridine adsorption of HPMoV@Mg_nAl-Surf (23) (n = 1-3) (a-c) and HPMoV@Mg₄Al-Surf (5-28) (d-h)

Fig. S11 IR spectra of HPMoV@Mg₄Al-Surf (5-28) (a-e) and HPMoV@Mg₄Al-Surf (5-28) (a1-e1) after absorption of 5-HMF

Fig. S12 The carbon balance for HPMoV, HPMoV@Mg₄Al-LDH (23) and HPMoV@Mg₄Al-Surf (5-28) for oxidation of 5-HMF. Reaction conditions: 100 mg of 5-HMF, 30 mg of catalyst, 4 mL of DMSO, 140 °C, 1.0 MPa of O₂, 12 h

Fig. S13 The generation of CO₂ was determined by GC-MS

Fig. S14 The content of DFF varied with time upon HPMoV, HPMoV@Mg₄Al-LDH (5-28) and HPMoV@Mg₄Al-Surf (5-28) at 140 °C with 1.0 MPa of O₂

Fig. S15 Oxidation of 5-HMF in different solvents under the reaction conditions of 100 mg of 5-HMF, 30 mg of catalyst, and 4 mL of solvent at 140 °C for 12 h with 1.0 MPa of O₂

Fig. S16 Oxidation of 5-HMF under different oxygen pressure. Reaction conditions: 100 mg of 5-HMF, 30 mg of catalyst, and 4 mL of DMSO at 140 °C for 12 h

Fig. S17 Optimization of reaction conditions on 5-HMF conversion at atmospheric O₂ (0.1 MPa) as (a) reaction temperature, (b) reaction time, (c) usage of catalyst on the oxidation of 5-HMF. Reaction conditions: 100 mg of 5-HMF, 4 mL of DMSO

Fig. S18 UV-Vis spectrum of the reaction mixture after separating HPMoV@Mg₄Al-Surf (23)

Fig. S19 The structure characterization of reused HPMoV@Mg₄Al-Surf (23). (a) DR-UV-vis, (b) IR, (c) ³¹P MAS NMR, (d) XPS, (e) SEM, and (f) HRTEM

Table S1 Oxidation of 5-HMF under various reaction conditions by different catalysts

Table S2 Elementary analysis, BET surface area, acid content and base content for HPMoV, Mg_nAl-LDH and HPMoV@Mg_nAl-Surf (n = 1-4)

Scheme S1 Reaction pathways for production of 5-HMF then to DFF from glucose in presence of multi-functional catalysts

S1. Materials

All chemicals and solvents were purchased from commercial supplies without further purification. In this paper, $\text{H}_5\text{PMo}_{10}\text{V}_2\text{O}_{40}$ (HPMoV) were prepared according to the well-established method^[1] and characterized by IR spectroscopy. $\text{Mg}_n\text{Al-LDH}$ (n represents Mg: Al = n : 1) with different proportions of magnesium and aluminum were synthesized according to Ref. [2].

S2. Physical measurements

The elemental analysis was determined by a Leeman Plasma Spec (I) ICP-ES. IR spectra ($4000\text{--}400\text{ cm}^{-1}$) were recorded on a Nicolet Magna 560 IR spectrometer (KBr disks). UV-vis spectra ($200\text{--}800\text{ nm}$) were performed on a Cary 500 UV-vis-NIR spectrophotometer. DR-UV-vis spectra ($200\text{--}800\text{ nm}$) were collected on a UV-2600 UV-vis spectrophotometer (Shimadzu). The structure of samples was characterized using a Japan Rigaku Dmax 2000 X-ray diffractometer with Cu $\text{K}\alpha$ radiation ($\lambda = 0.154178\text{ nm}$). The ^{31}P MAS NMR were acquired by using a Bruker AM500 spectrometer at 202.5 MHz. XPS spectra were recorded on an Escalab-MK II photoelectronic spectrometer equipped with a micro-focus monochromatic Al $\text{K}\alpha$ X-ray source. SEM micrographs and EDX spectra were obtained using a XL30 ESEM FEG at 25 kV (PhilipsXL-30). EDX was carried out to prove the existence of the Mg, Al, O, P, Mo and V elements. TEM micrographs were measured on a JEM-2100F instrument. Nitrogen adsorption-desorption isotherms and Brunauer-Emmet-Teller (BET) surface area were measured using an ASAP 2010M surface analyzer (the samples were degassed at $100\text{ }^\circ\text{C}$ overnight). The acidic and basic properties were detected by a ZDJ-4B automatic potentiometric titrator. The product analysis was detected by using a high-performance liquid chromatography (HPLC) that equipped with a reversed-phase C18 column and a UV detector at the wavelength of 278 nm. Acetonitrile and ultrapure water (V/V = 2: 1) were used as mobile phase with a flow rate of 0.8 mL/min. The total organic carbon (TOC) was measured by a TOC Analyzer (TOC-LCPH, Shimadzu, Japan).

S3. Aerobic oxidation of 5-HMF

Aerobic oxidation of 5-HMF was carried out in Teflon-lined autoclave equipped with a magnetic stirrer. Typically, 100 mg of 5-HMF and 30 mg of catalyst were added into 4 mL of DMSO, then the mixture was heated up to $140\text{ }^\circ\text{C}$. During the reaction, the reactor was maintained at 1.0 MPa of oxygen pressure. After the reaction, the reactor was cooled to room temperature. The catalyst was separated from the mixture by centrifuge, then washed with ethanol several times and dried

in oven at 60 °C for 12 h for reuse. Meanwhile, the reused experiment was carried out as the catalyst was separated by centrifuge and reused without any treatment.

$$\text{5-HMF conversion} = \text{moles of converted 5-HMF} / \text{moles of initial 5-HMF} \times 100 \%$$

$$\text{DFF yield} = \text{moles of DFF} / \text{moles of initial 5-HMF} \times 100 \%$$

S4. Aerobic oxidation of fructose or glucose

Aerobic oxidation of fructose or glucose was carried out in Teflon-lined autoclave equipped with a magnetic stirrer. In the experiment, fructose or glucose (100 mg) and catalyst (30 mg) were added to 4 mL of DMSO, and the mixture was heated up to 140 °C under 0.8 MPa of O₂. After the reaction, the reactor was cooled to room temperature, then the reused experiment was carried out in accordance with the above method in S3.

S5. Determination of the acidic and basic properties

The total acid content of catalysts was determined by automatic potentiometric titration. 50 mg catalyst was suspended in 50 mL of acetonitrile with stirring vigorously for 3 h. Then the resulting mixture was titrated with the solution of n-butylamine in acetonitrile (0.01 M). The titration endpoint could be detected from the potentiometric titration curve and the total acid content of the catalysts could be calculated. IR spectra of pyridine adsorption was used for recognizing the Lewis and Brønsted acid sites. Pyridine was adsorbed by catalysts for 12 h under the condition of vacuum and 60 °C. The capacity of acidity was calculated by Lambert-Beer formula: $A = (\epsilon \times W \times c) / S$. (A: absorbance, cm⁻¹, ϵ : extinction coefficient, m²·mol⁻¹, W: the sample weight, kg, c: the concentration of acid, mmol·g⁻¹, S: the sample disk area, m²). The amount of Lewis and Brønsted acid sites was estimated from the integrated area of the adsorption bands at 1450 and 1540 cm⁻¹, respectively. The base content of the catalysts was measured by using the conductivity titration method. 50 mg catalyst was suspended in 50 mL of diluted 0.001 M HCl with stirring vigorously for 3 h. Then the resulting mixture was titrated with the solution of 0.01 M NaOH. The titration endpoint could be detected by a sudden increase in conductivity.

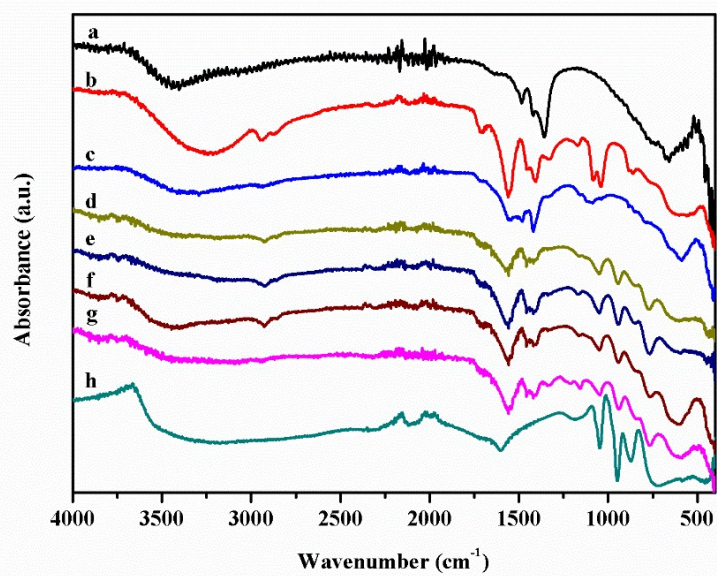


Fig. S1 IR spectra of Mg₄Al-LDH (a), Mg₄Al-COOH (b), Mg₄Al-NH₂ (c), HPMoV@Mg₁Al-Surf (23) (d), HPMoV@Mg₂Al-Surf (23) (e), HPMoV@Mg₃Al-Surf (23) (f), HPMoV@Mg₄Al-Surf (23) (g), and HPMoV (h)

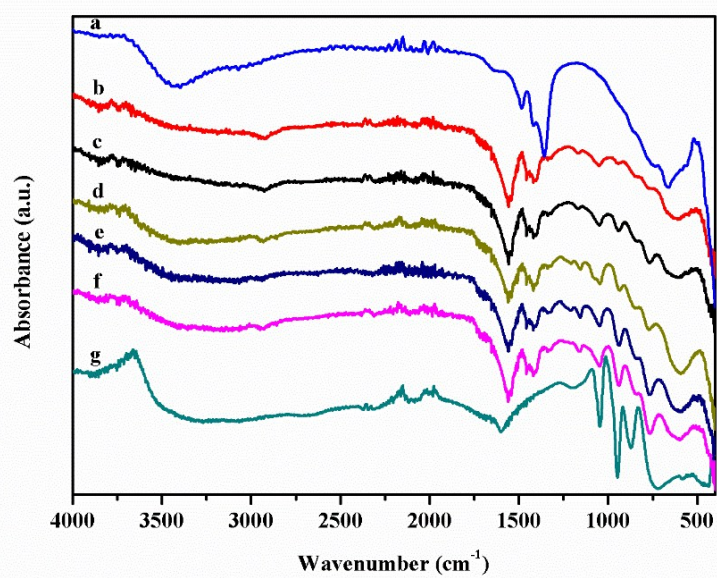


Fig. S2 IR spectra of HPMoV@Mg₄Al-Surf with different loading amount: Mg₄Al-LDH (a), HPMoV@Mg₄Al-Surf (5) (b), HPMoV@Mg₄Al-Surf (12) (c), HPMoV@Mg₄Al-Surf (17) (d), HPMoV@Mg₄Al-Surf (23) (e), HPMoV@Mg₄Al-Surf (28) (f), and HPMoV (g)

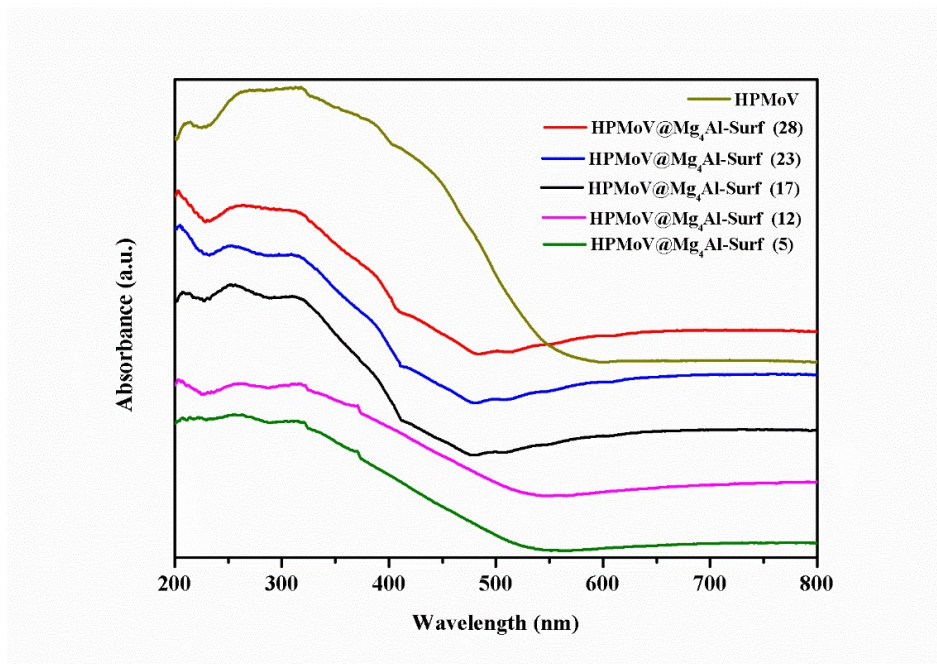


Fig. S3 DR-UV-vis spectra of the HPMoV@Mg₄Al-Surf (5-28)

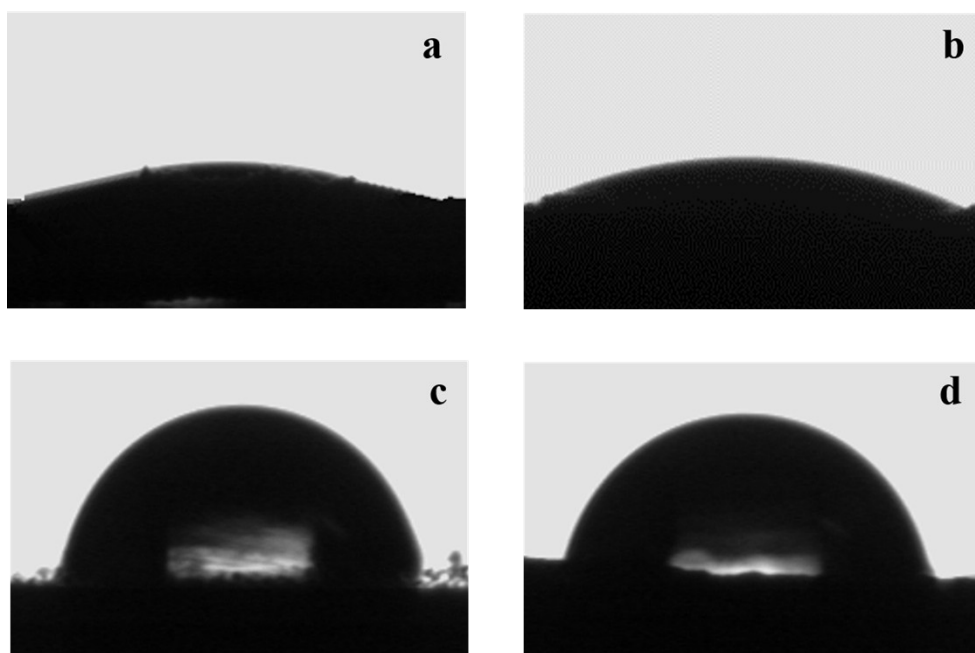


Fig. S4 Water contact angle of Mg_4Al -LDH (a), Mg_4Al-NH_2 (b), Mg_4Al -Surf (c) and $HPMoV@Mg_4Al$ -Surf (23) (d)

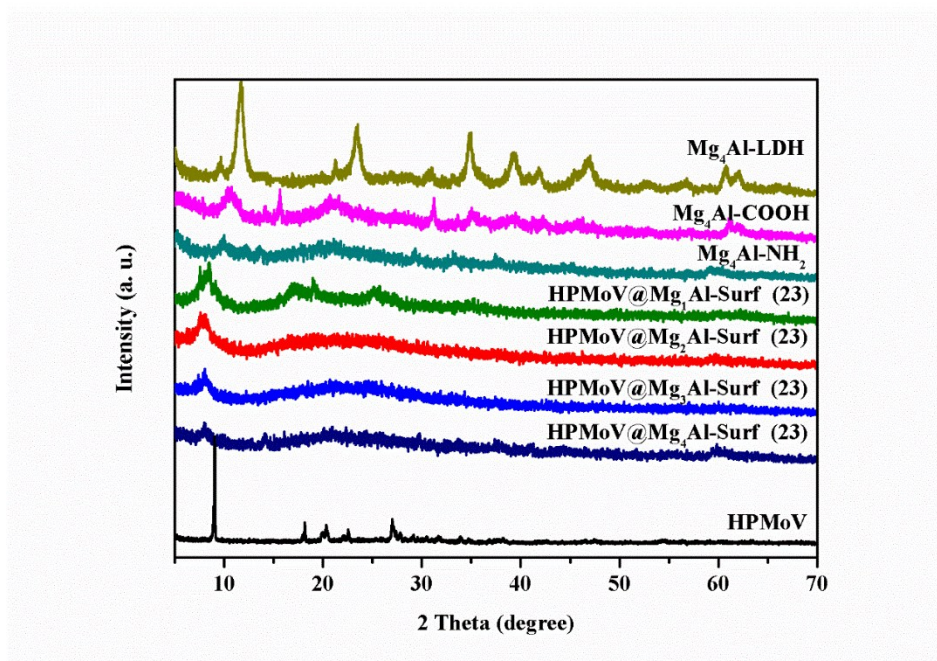


Fig. S5 XRD patterns of Mg₄Al-LDH, Mg₄Al-COOH, Mg₄Al-NH₂, HPMoV@Mg_nAl-Surf (23) (n = 1, 2, 3, 4) and HPMoV

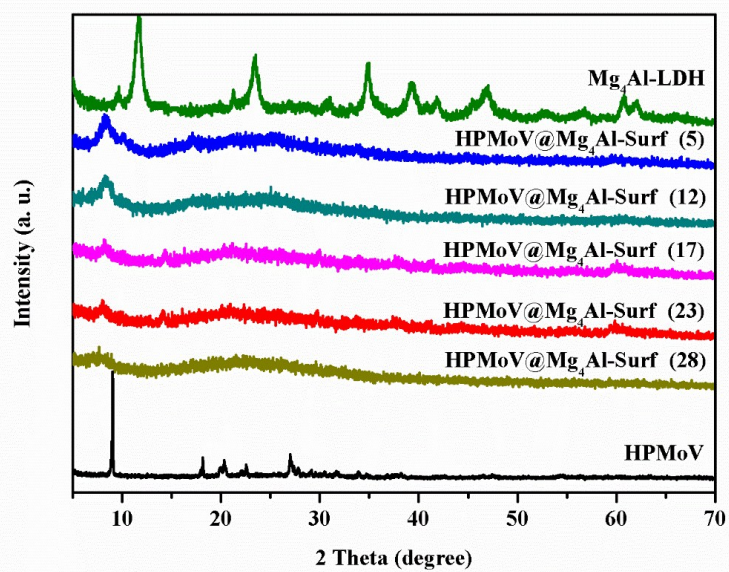


Fig. S6 XRD patterns of Mg₄Al-LDH, HPMoV@Mg₄Al-Surf (5-28) and HPMoV

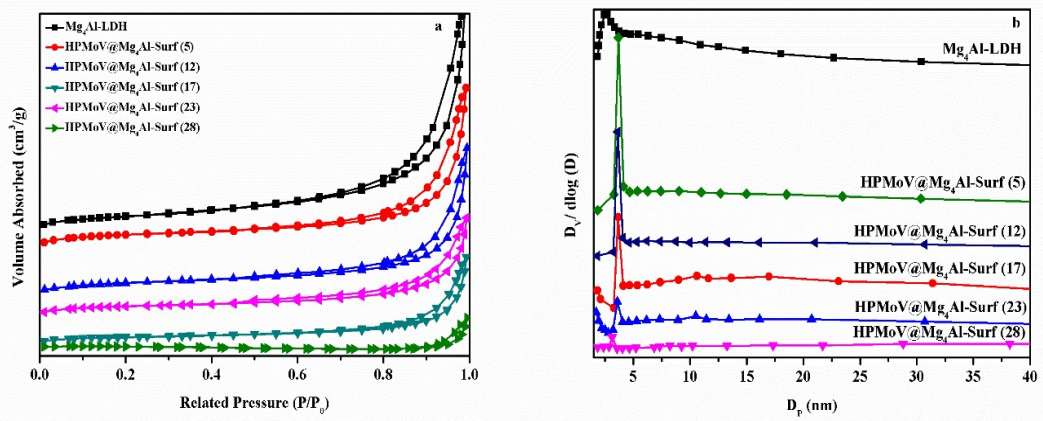


Fig. S7 Nitrogen adsorption-desorption isotherms (a) and pore size distribution profiles according to BJH desorption dV/dD pore volume (b) of Mg₄Al-LDH and HPMoV@Mg₄Al-Surf (5-28)

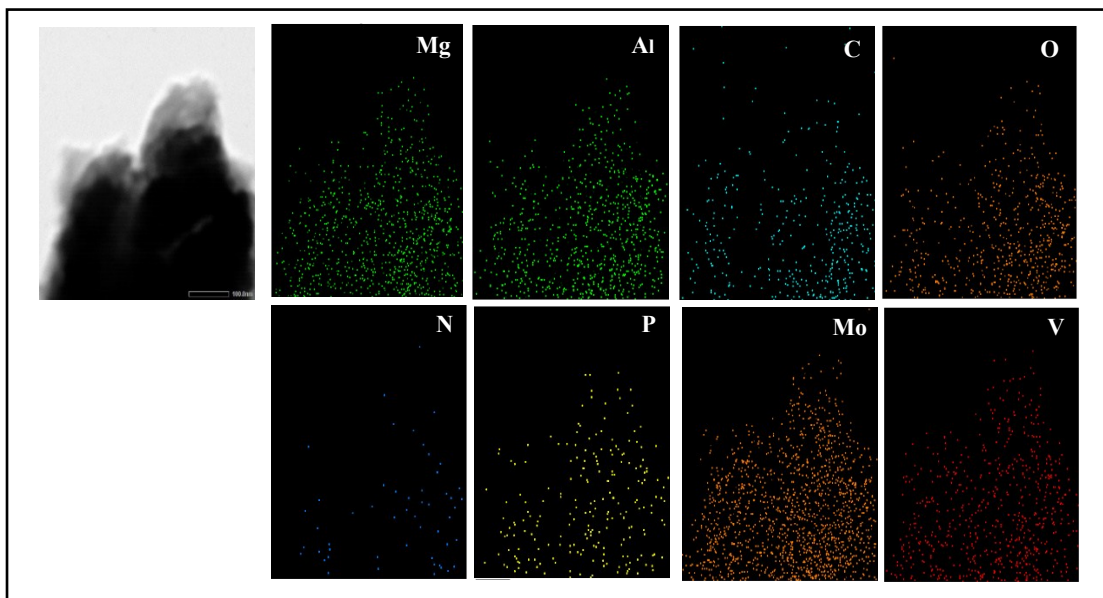


Fig. S8 The Energy-dispersive spectroscopy (EDX) mapping of HPMoV@Mg₄Al-Surf (23)

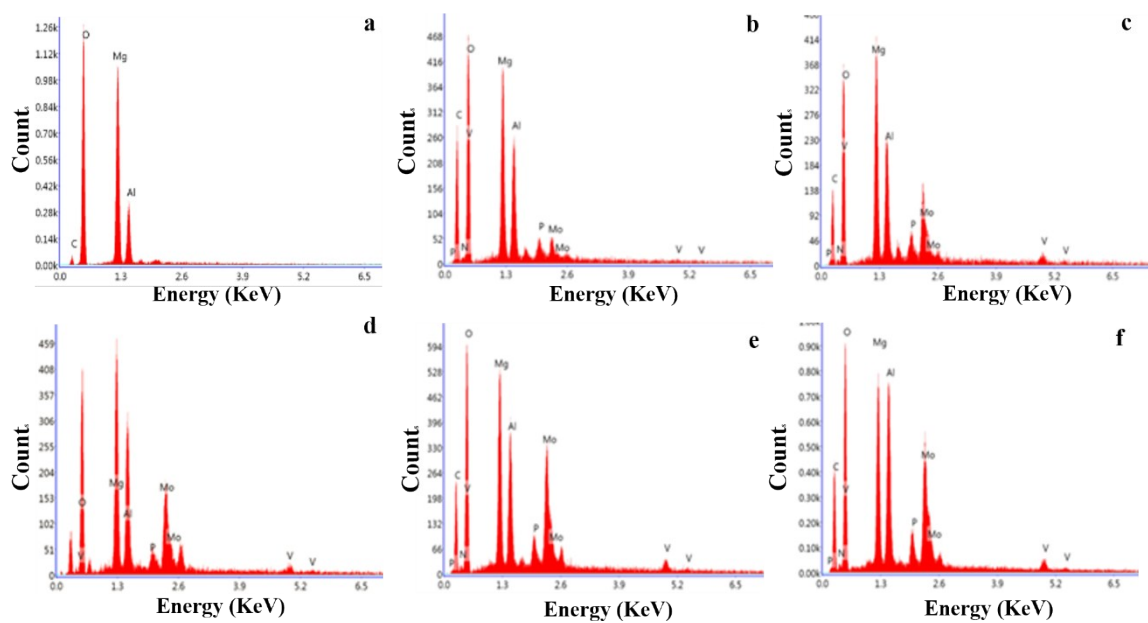


Fig. S9 The EDAX of Mg₄Al-LDH (a) and HPMoV@Mg₄Al-Surf (5-28) (b-f)

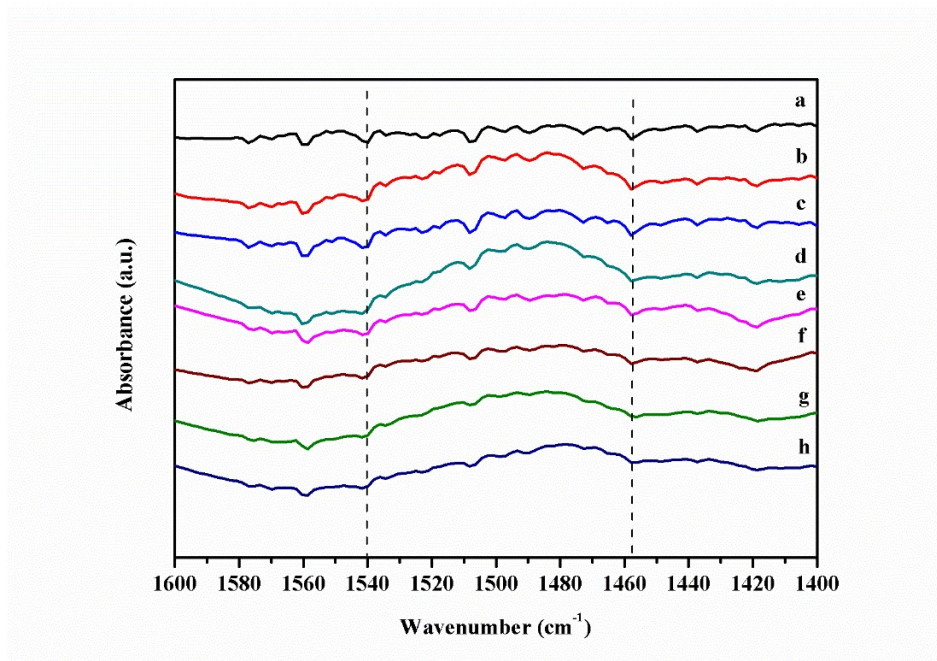


Fig. S10 IR spectra of pyridine adsorption of HPMoV@Mg_nAl-Surf (23) (n = 1-3) (a-c) and HPMoV@Mg₄Al-Surf (5-28) (d-h)

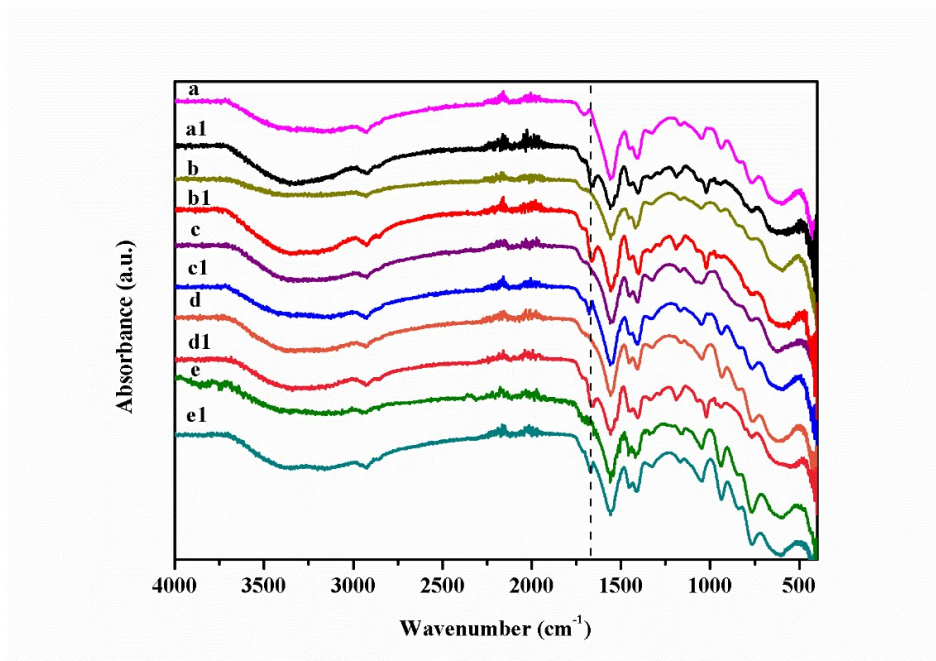


Fig. S11 IR spectra of HPMoV@Mg₄Al-Surf (5-28) (a-e) and HPMoV@Mg₄Al-Surf (5-28) (a1-e1) after absorption of 5-HMF

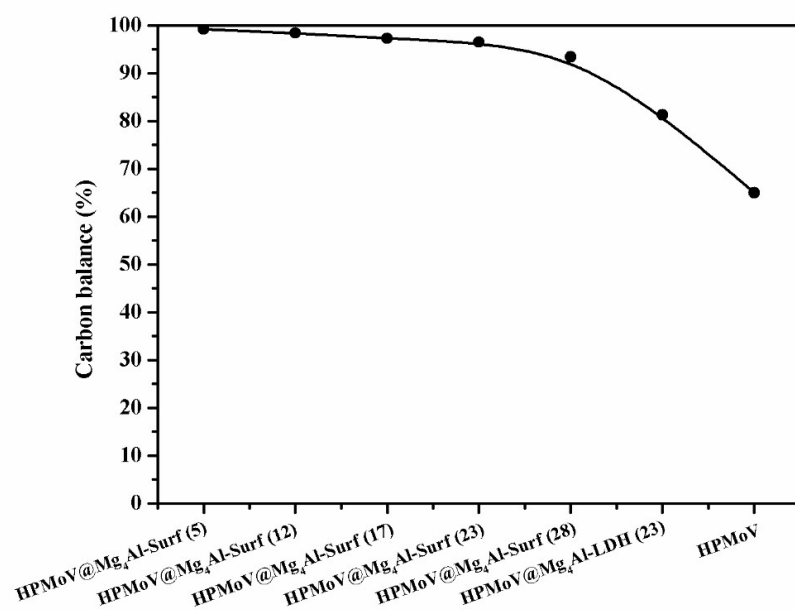


Fig. S12 The carbon balance for HPMoV, HPMoV@Mg₄Al-LDH (23) and HPMoV@Mg₄Al-Surf (5-28) for oxidation of 5-HMF. Reaction conditions: 100 mg of 5-HMF, 30 mg of catalyst, 4 mL of DMSO, 140 °C, 1.0 MPa of O₂, 12 h

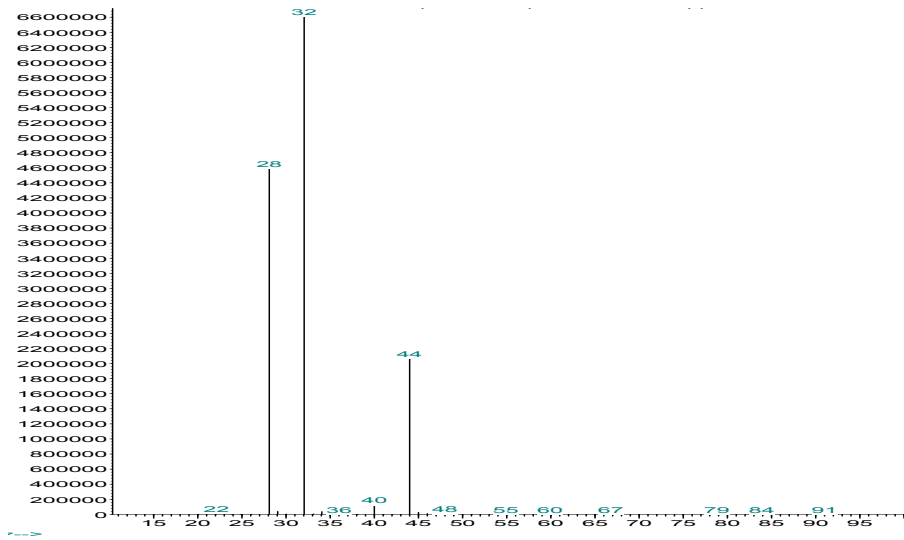


Fig. S13 The generation of CO₂ was determined by GC-MS

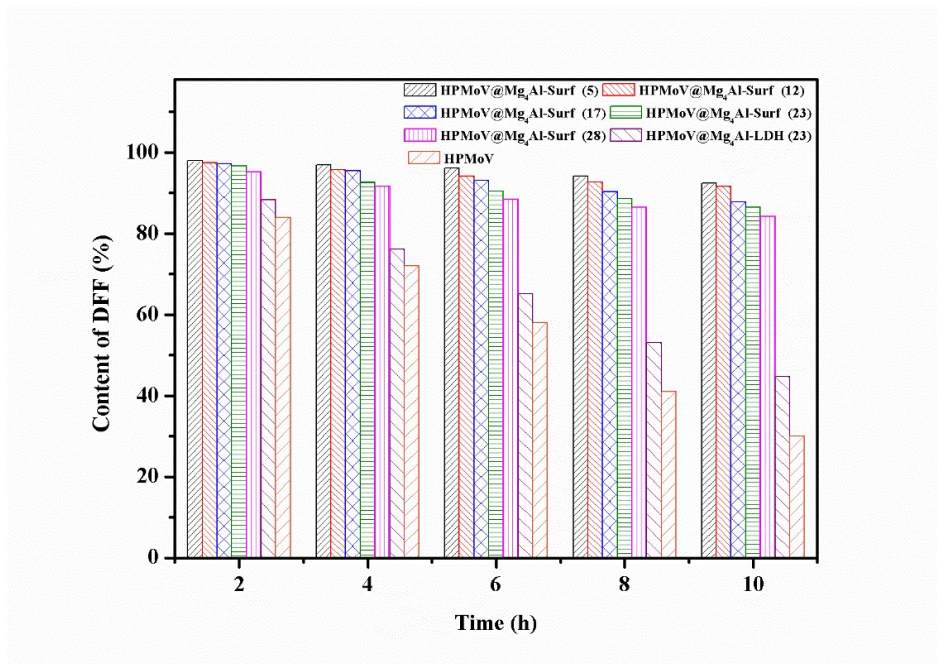


Fig. S14 The content of DFF varied with time upon HPMoV, HPMoV@Mg₄Al-LDH (5-28) and HPMoV@Mg₄Al-Surf (5-28) at 140 °C with 1.0 MPa of O₂

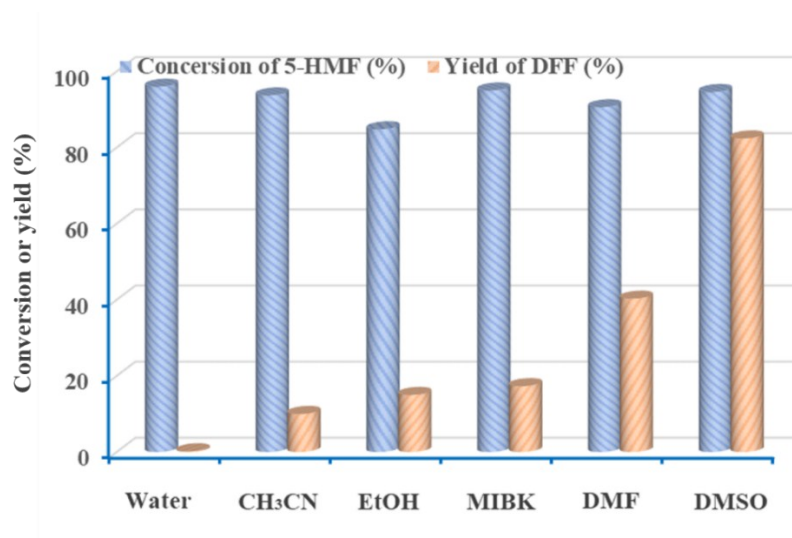


Fig. S15 Oxidation of 5-HMF in different solvents under the reaction conditions of 100 mg of 5-HMF, 30 mg of catalyst, and 4 mL of solvent at 140 °C for 12 h with 1.0 MPa of O₂

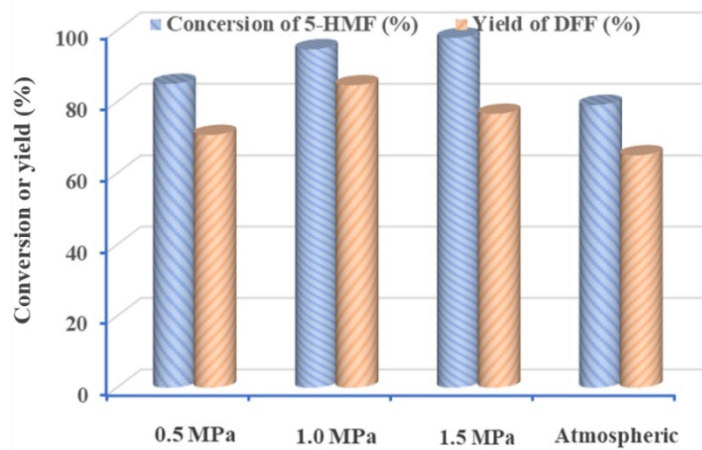


Fig. S16 Oxidation of 5-HMF under different oxygen pressure. Reaction conditions: 100 mg of 5-HMF, 30 mg of catalyst, and 4 mL of DMSO at 140 °C for 12 h

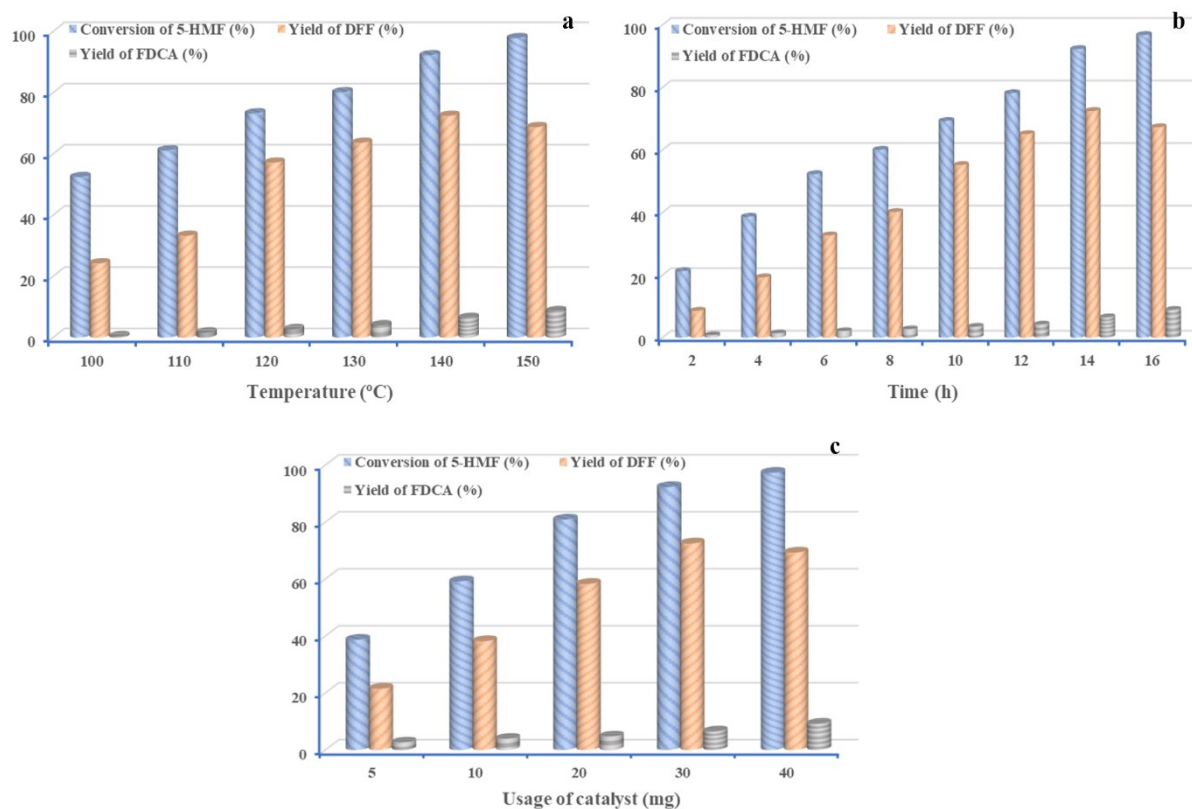


Fig. S17 Optimization of reaction conditions on 5-HMF conversion at atmospheric O₂ (0.1 MPa) as (a) reaction temperature, (b) reaction time, (c) usage of catalyst on the oxidation of 5-HMF.

Reaction conditions: 100 mg of 5-HMF, 4 mL of DMSO

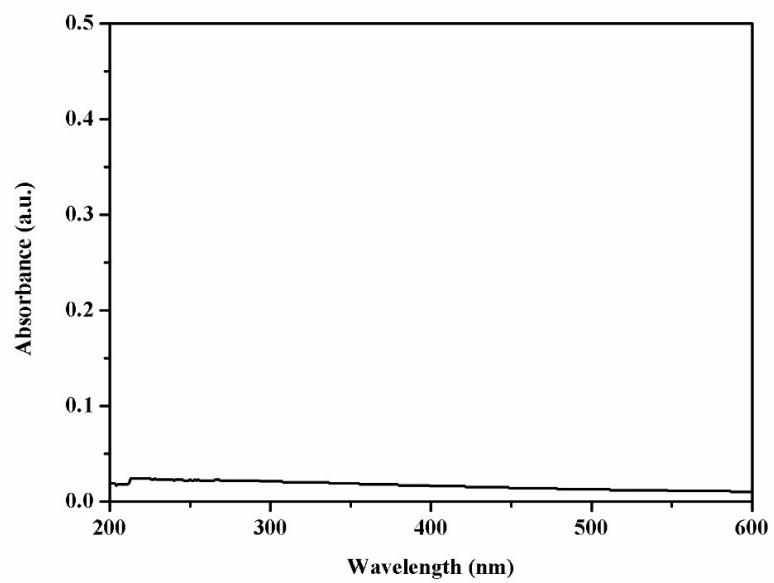


Fig. S18 UV-Vis spectrum of the reaction mixture after separating HPMoV@Mg₄Al-Surf (23)

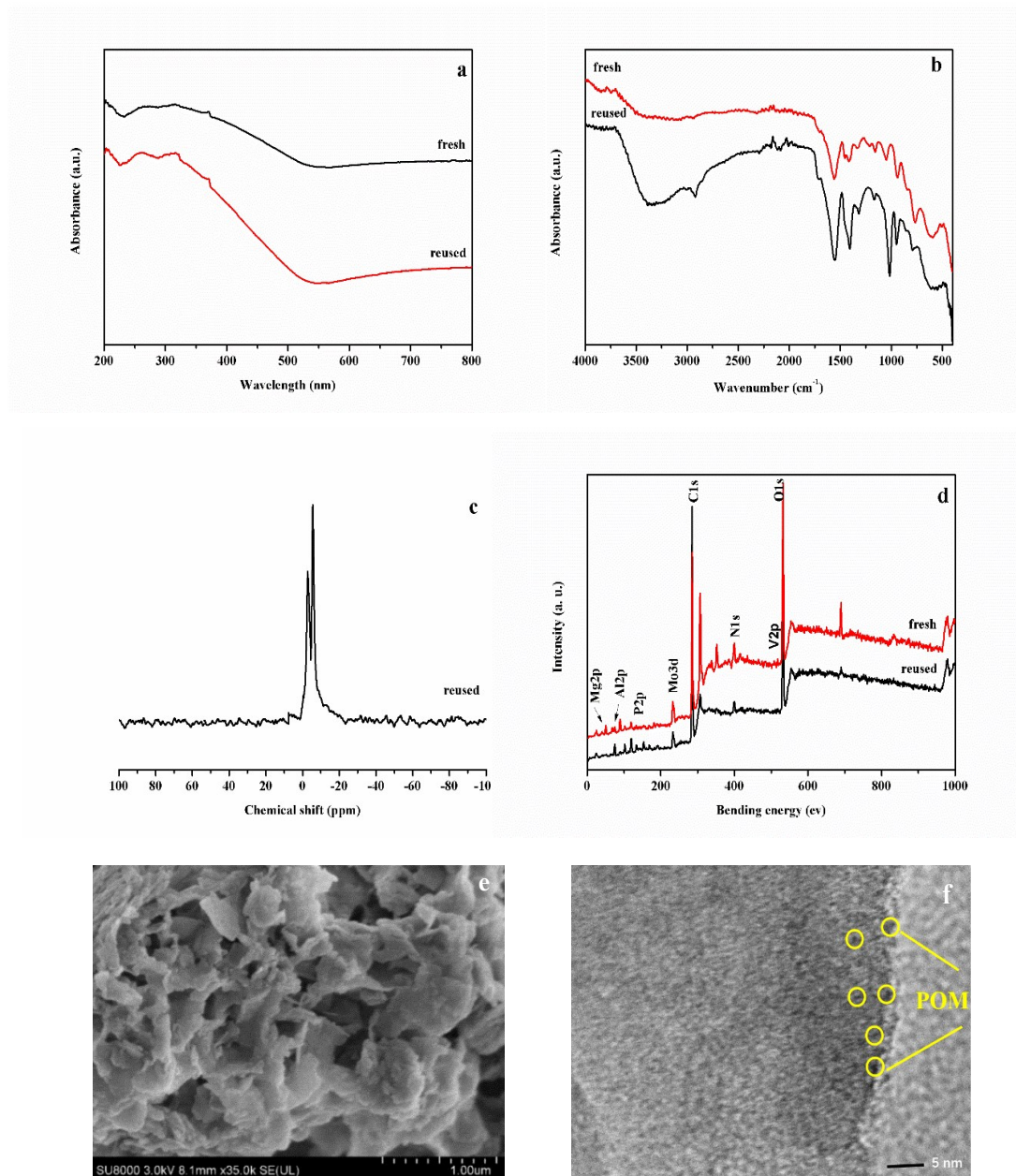


Fig. S19 The structure characterization of reused HPMoV@Mg₄Al-Surf (23). (a) DR-UV-vis, (b) IR, (c) ³¹P MAS NMR, (d) XPS, (e) SEM, and (f) HRTEM

Table S1 Oxidation of 5-HMF under various reaction conditions by different catalysts

Catalysts	Reaction Condition	Oxidant	T (°C)	Time (h)	Con.%	Yield of DFF %	Yield of FDCA%	Yield of FFCA%	Ref.
Mn ₆ Fe ₁ O _x	1 mmol HMF, 5 mL DMF	O ₂ 1.5 MPa	110	5	97	91	-	-	3
Co-Mn/N@C	0.5 mmol HMF, 10 mL H ₂ O	O ₂ 1 bar	85	12	99.7	-	96.1	-	4
Cs/MnO _x	63 mg HMF, 10 mL DMF	O ₂ 10 bar	100	12	98.4	94.7	-	-	5
Au/HAP	0.2513 g HMF, 20 mL CH ₃ OH	Air 2.4 MPa	130	6	99.1	-	89.3	-	6
Pt/Fe ₃ O ₄ /rGO	0.50 mmol HMF, 20 mL H ₂ O	O ₂ 0.5 MPa	95	0.5	100	-	98	-	7
MnO _x /P25 (TiO ₂)	1mmol 5-HMF, 10 g ethanol	Air 30 bar	140	2	33	32	-	-	8
Pd-Au/HT (1 : 4)	200 mg HMF, 50 ml H ₂ O	O ₂ 60 mL/min.	60	6	99.9	-	90	-	9
Pt/PVP	0.5 mmol HMF, 10 mL H ₂ O	O ₂ 1.0 MPa	110	5	99.9	-	99.9	-	10
Au/CeO ₂	0.5 mmol HMF, 20 ml H ₂ O	O ₂ 0.5 MPa	130	2.5	99.9	-	90	-	11
Pd/CC	0.1 g HMF, 5 mL H ₂ O	O ₂ 20 mL/min	140	30	93	-	85	-	12
MgO-CeO ₂	0.14 M 5-HMF, 7 mL H ₂ O	O ₂ 0.9 bar	100	9	97.8	96	-	-	13
Ru/AC	0.3 mmol HMF, 14.5 mL H ₂ O,	O ₂ 1 bar	75,	1	100	-	-	92	14
Au-Ru/rGO	0.5 mmol of HMF, 10 ml toluene,	O ₂ 5 bar	80	8	90.9	-	-	95.7	15
Pt-Ni/AC-15ALD	0.015 g HMF, 3 mL H ₂ O	O ₂ 0.8 MPa	100	15	100	-	97.5	-	16
NiFe-LDH	10 mmol HMF, 1M KOH	-	25	1.5	98	-	98	-	17
NC-T	0.5 mmol HMF, 10 mL acetonitrile	O ₂ 10 bar	100	4	100	95.1	-	-	18
Ru/ZrO ₂	0.5 mmol HMF, 10 mL H ₂ O	O ₂ 10 bar	120	16	100	-	97	3	19
	2 mmol HMF	O ₂		24					

MnCo ₂ O ₄	15 mL toluene	1.0 MPa							
Fe ₃ O ₄ @SiO ₂	0.4 mmol HMF, 5 mL H ₂ O	O ₂ 10 bar	110	48	92	-	73.6	-	21
MnCo ₂ O ₄	0.2 mmol HMF, 5 mL H ₂ O	O ₂ 1 MPa	100	24	99.9	-	70.9	-	22
MnFe ₂ O ₄	1 mmol HMF, 20 ml acetonitrile	-	100	5	99	-	85	-	23
Cu/NG, TEMPO	126 mg HMF, 15 mL acetonitrile	O ₂ 0.4 MPa	70	8	99.8	99.2	-	-	24
MgO·MnO ₂ ·C eO ₂	0.015 M 5-HMF, 7 mL of H ₂ O	O ₂ 2.0 MPa	110	10	98.9	-	94	-	25
CoPz/g-C ₃ N ₄	100.8 mg HMF, 40 mL buffer solution	Air 20 mL/min	25	14	99.6	-	96.1	-	26
ZnFe _{1.65} Ru _{0.35} O ₄	0.5 mol HMF, 3 mL DMF	O ₂ 20 mL/min	110	4	94	82.2	3.4	-	27
Ru/MnCo ₂ O ₄	2 mmol HMF, 20 mL H ₂ O	Air 0.7 MPa	120	10	100	-	99.1	-	28
Ni _{0.9} Pd _{0.1}	2 mmol HMF, 10 mL H ₂ O	O ₂ 1.0 MPa	80	4	>99	-	86	-	29
Co/Mn/Br	2.2-2.3 mmol HMF, 2.5 mL HOAc	O ₂ 0.76 MPa	180	1/6	>99	-	92.9	-	30
α-CuV ₂ O ₆	1mol HMF, 4 mL DMSO	O ₂ 1 bar	130	3	100	99.9	-	-	31
V ₂ O ₅ /ceramic	63 mg HMF, 4 mL DMSO	O ₂ 40 mL/min	140	5	100	87.5	-	-	32
MnO ₂	0.2 mmol HMF, 5 mL H ₂ O	O ₂ 1.0 MPa	100	24	≥99	-	91	-	33
CC-SO ₃ H-NH ₂	200 mg HMF, 2 mL DMSO	O ₂ 20 mL/min	140	9	85	85	-	-	34
PMA-MIL-101	0.5 mol HMF, 5 mL DMSO	O ₂ 20 mL/min	140	20	90.8	88.2	-	-	35
SBA-15- Biimidazole- Ru	0.5 mol HMF 8 mL 4- chlorotoluene	O ₂ 20 mL/min	110	11	96.9	88.7	-	-	36
Ru/C	1 mmol HMF, 10 mL H ₂ O	O ₂ 0.5 MPa	120	10	100	-	88	-	37
Au-Pd/ZOC	0.5 mmol HMF, 10 mL H ₂ O	O ₂ 3 bar	80	4	>99	-	>99	-	38

Pd/HT-5	0.4 mmol HMF, 10 mL H ₂ O	O ₂ 100mL/min	100	8	100	–	99	–	39
Fe ₃ O ₄ @C @Pt	15 mg HMF, 0.2 mmol Na ₂ CO ₃	O ₂ 100mL/min	90	4	100	–	100	–	40
Pt/C-O-Mg	0.5 mmol HMF, 10 mL H ₂ O	O ₂ 1.0 MPa	110	12	100	–	97	–	41
FeCo/C	1mol HMF, 2 mL toluene	O ₂ 1.0 MPa	100	6	99	99	–	–	42
Co/Mn/Br	13.2 mmol 5- HMF, 5 mL HOAc	N ₂ /O ₂ = 1/1 (mol/mol)	160	0.5	100	–	78.1	–	43
Bi(NO ₃) ₃ ·5H ₂ O, cellulose- Cu-NP	126 mg HMF, 10 mL MeCN	Air	80	2	96.5	82	–	–	44
Ni ₃ (BTP) ₂	1.8 mmol HMF, 25 mL H ₂ O	O ₂ 30 bar	120	24	100	99	–	–	45
SBA-NH ₂ -VO ²⁺ SBA-NH ₂ -Cu ²⁺	100 mg HMF 7 mL 4- chlorotoluene	O ₂ 0.28 MPa	110	12	98.8	62.7	–	–	46
V ₂ O ₅	2.0 mmol HMF 10 mL acetic acid	O ₂ 10 bar	100	4	99	–	–	75	47
N-doped graphene NG-800	1mol HMF, 30 mL acetonitril	O ₂ 1.0 MPa	100	6	100	99.5	–	–	48
NNC-900	0.63 mmol HMF, 10 mL H ₂ O	O ₂ 100mL/min	80	48	100	–	80	–	49
GO	2 mmol HMF, 4 mL DMSO	O ₂ 20 mL/min	140	24	100	90	–	–	50
[EMIM] ₄ Mo ₈ O ₂₆	9 mmol HMF, 18 mmol NaOH 20 mL H ₂ O	25 ml 6 % H ₂ O ₂	100	2	96.2	–	92.7	–	51
Ru/CTF	1mmol HMF, 15 mL MTBE	Air 20 bar	80	1	86.3	63.6	–	–	52
Ru/CTF	1mmol HMF, 15 mL H ₂ O	Air 20 bar	140	3	100	0.1	77.6	–	53
C-Fe ₃ O ₄ -Pd	0.4 mmol HMF, 8 mL H ₂ O	O ₂ 30 mL/min	80	4	98.2	–	91.8	–	54
Pt/TiO ₂	2 g HMF, NaHCO ₃ /5- HMF=2	Air 0.1 MPa	100	6	>99.9	–	>99.9	–	55
Pt/CNT	0.5 mmol HMF,	O ₂	90	14	100	–	98	–	56

	20 ml H ₂ O	0.5 MPa							
Polyaniline-VO(acac) ₂	100 mg HMF, 8 mL 4-chlorotoluene	O ₂ 20 mL/min	110	12	99.2	86.2	-	-	57
VO ₂ -PANI/CNT	1mol HMF, 2 mL DMSO	O ₂ 1.0 MPa	120	11	>99	96	-	-	58
Fe ₃ O ₄ -CoO _x	70 mg HMF, 4 mL DMSO	t-BuOOH 0.5 mL	80	15	97.2	-	68.6	-	59
GO	1mol HMF, 30 mL acetonitrile	-	100	18	100	99.6	-	-	60
GO _{ase} M ₃₋₅ PaoABC	0.3 mmol 5-HMF, 0.3 mL MeCN	Air 1.0 MPa	37	10	100	-	86.9	-	61
Cs ₃ HPMo ₁₁ VO ₄₀	1mol 5-HMF, 2 mL DMSO	O ₂ 0.8 MPa	110	6	99	99	-	-	62
Au-Pd/CNT	0.50 mmol HMF, 20 mL H ₂ O	O ₂ 0.5 MPa	100	12	99	-	99	-	63
Ag-OMS-2	315 mg HMF, 40 mL isopropyl alcohol	Air 15 atm	165	6	99	99	-	-	64
FeIII-POP-1	1.58 mmol HMF, 10 mL H ₂ O	Air 10 bar	100	10	100	-	79	-	65
K-OMS-2	100 mg HMF, 3 mL DMSO	O ₂ 10 mL/min	110	6	99	99	-	-	66
Au/HT	1 mmol HMF, 6 mL H ₂ O	O ₂ 50 mL/min	95	7	99	-	99	-	67
Fe ₃ O ₄ /Mn ₃ O ₄	126 mg HMF, 7 mL DMF	O ₂ 20 mL/min	120	4	99.8	82.1	-	-	68
RuCo(OH) ₂ -CeO ₂	126 mg HMF, 7 mL MIBK	O ₂ 20 mL/min	120	12	96.5	82.6	8.9	-	69
Ru/hydroxyapatite	100 mg HMF, 7 mL 4-chlorotoluene	O ₂ 20 mL/min	90	4	100	89.1	9.3	-	70

Table S2 Elementary analysis, BET surface area, acid content and base content for HPMoV, Mg_nAl-LDH and HPMoV@Mg_nAl-Surf (n = 1-4)

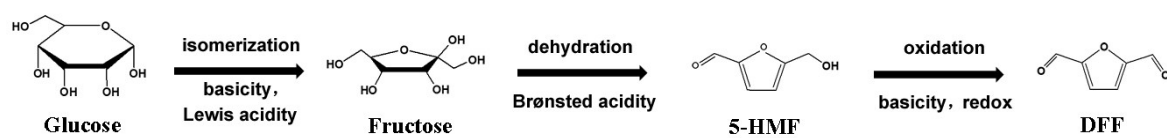
Catalyst	Elementary results (calculated values in parenthesis) ^a /%					Loading amount wt %	S _{BET} (m ² /g)	Acidity (mmol/g)			Basicity ^d (mmol/g)
	P	Mo	V	Al	Mg			Total acidity ^b (mmol/g)	B-acidity ^c (mmol/g)	L-acidity ^c (mmol/g)	
HPMoV	1.80	55.20	5.85	-	-	-	3.90	2.66	2.60	-	-
Mg ₁ Al-LDH	-	-	-	18.03	16.31	-	78.5	0.21	-	0.20	0.68
Mg ₂ Al-LDH	-	-	-	13.02	23.38	-	75.4	0.18	-	0.17	0.74
Mg ₃ Al-LDH	-	-	-	10.09	27.45	-	71.2	0.16	-	0.14	0.86
Mg ₄ Al-LDH	-	-	-	8.31	30.00	-	68.6	0.12	-	0.11	0.94
HPMoV@Mg ₁ Al-Surf (23)	0.59	18.04	1.93	8.82	7.95	23.0	36.0	0.73	0.51	0.16	0.11
HPMoV@Mg ₂ Al-Surf (23)	0.63	19.98	2.13	4.92	8.83	23.0	32.6	0.70	0.50	0.14	0.13
HPMoV@Mg ₃ Al-Surf (23)	0.59	18.70	2.01	4.63	12.35	23.0	29.5	0.67	0.51	0.11	0.14
HPMoV@Mg ₄ Al-Surf (5)	0.19	5.42	0.54	6.10	21.92	5.0	45.4	0.21	0.08	0.10	0.56
HPMoV@Mg ₄ Al-Surf (12)	0.38	11.39	0.23	5.38	19.25	12.0	38.0	0.37	0.22	0.09	0.42
HPMoV@Mg ₄ Al-Surf (17)	0.49	14.85	1.57	4.95	17.76	17.0	33.6	0.47	0.34	0.08	0.28
HPMoV@Mg ₄ Al-Surf (23)	0.57	18.35	1.98	4.52	16.19	23.0	23.4	0.62	0.51	0.07	0.20
HPMoV@Mg ₄ Al-Surf (28)	0.71	20.85	2.23	4.21	15.08	28.0	13.4	0.68	0.57	0.06	0.13

^aThe elementary results were calculated by the ICP-AES.

^bThe total acidity was measured by potentiometric titration.

^cThe B and L acidity were valued by the IR spectra of adsorbed pyridine and calculated by Lambert-Beer equation.

^dThe basicity was measured by conductivity titration method.



Scheme S1 Reaction pathways for production of 5-HMF then to DFF from glucose in presence of multi-functional catalysts

Reference

1. G. A. Tsigdinos and C. J. Hallada, *Inorg. Chem.*, 1968, **7**, 437-441.
2. D. G. Cantrell, L. J. Gillie, A. F. Lee and K. Wilson, *Appl. Catal. A: Gen.*, 2005, **287**, 183-190.
3. H. Liu, X. J. Cao, J. N. Wei, W. L. Jia, M. Z. Li, X. Tang, X. H. Zeng, Y. Sun, T. Z. Lei, S. J. Liu and L. Lin, *ACS Sustainable Chem. Eng.*, 2019, **7**, 7812-7822.
4. H. Zhou, H. H. Xu and Y. Liu, *Appl. Catal. B: Environ.*, 2019, **244**, 965-973.
5. Z. L. Yuan, B. Liu, P. Zhou, Z. H. Zhang and Q. Chi, *Catal Sci Technol.*, 2018, **8**, 4430-4439.
6. D. K. Mishra, J. K. Cho, Y. J. Yi, H. J. Lee and Y. J. Kim, *J. Ind. Eng. Chem.*, 2019, **70**, 338-345.
7. C. M. Zhou, W. R. Shi, X. Y. Wan, Y. Meng, Y. Yao, Z. Guo, Y. H. Dai, C. Wang and Y. H. Yang, *Catal. Today*, 2019, **330**, 92-100.
8. L. F. Chen, W. Y. Yang, Z. Y. Gui, S. Saravanamurugan, A. Riisager, W. R. Cao and Z. W. Qi, *Catal. Today*, 2019, **319**, 105-112.
9. H. A. Xia, J. H. An, M. Hong, S. Q. Xu, L. Zhang and S. L. Zuo, *Catal. Today*, 2019, **319**, 113-120.
10. H. J. Yu, K. A. Kim, M. J. Kang, S. Y. Wang and H. G. Cha, *ACS Sustain. Chem. Eng.*, 2018, **7**, 3742-3748.
11. Q. Q. Li, H. Y. Wang, Z. P. Tian, Y. J. Weng, C. G. Wang, J. R. Ma, C. F. Zhu, W. Z. Li, Q. Y. Liu and L. L. Ma, *Catal. Sci. Technol.*, 2019, **9**, 1570-1580.
12. P. V. Rathod and V. H. Jadhav, *ACS Sustain. Chem. Eng.*, 2018, **6**, 5766-5771.
13. M. Ventura, F. Lobefaro, E. De Giglio, M. Distaso, F. Nocito and A. Dibenedetto, *ChemSusChem*, 2018, **11**, 1305-1315.
14. C. T. Chen, C. V. Nguyen, Z. Y. Wang, Y. Bando, Y. Yamauchi, M. T. S. Bazziz, A. Fatehmulla, W. A. Farooq, T. Yoshikawa, T. Masuda and K. C. W. Wu, *ChemCatChem*, 2018, **10**, 361-365.
15. B. Ma, Y. Y. Wang, X. N. Guo, X. L. Tong, C. Liu, Y. W. Wang and X. Y. Guo, *Appl. Catal. A: Gen.*, 2018, **552**, 70-76.
16. J. S. Shen, H. Chen, K. Q. Chen, Y. Qin, X. Y. Lu, P. K. Ouyang and J. Fu, *Ind. Eng. Chem. Res.*, 2018, **57**, 2811-2818.
17. W. J. Liu, L. N. Dang, Z. R. Xu, H. Q. Yu, S. Jin and G. W. Huber, *ACS Catal.*, 2018, **8**, 5533-5541.
18. Y. S. Ren, Z. L. Yuan, K. L. Lv, J. Sun, Z. H. Zhang and Q. Chi, *Green Chem.*, 2018, **20**, 4946-4956.
19. C. M. Pichler, M. G. Al-Shaal, D. Gu, H. Joshi, W. Ciptonugroho and F. Schuth, *ChemSusChem*, 2018, **11**, 2083-2090.

20. D. K. Mishra, J. K. Cho and Y. J. Kim, *J. Ind. Eng. Chem.*, 2018, **60**, 513-519.
21. A. Tirsoaga, M. El Fergani, V. I. Parvulescu and S. M. Coman, *ACS Sustain. Chem. Eng.*, 2018, **6**, 14292-14301.
22. S. Zhang, X. Sun, Z. Zheng and L. Zhang, *Catal. Commun.*, 2018, **113**, 19-22.
23. A. B. Gawade, A. V. Nakhate and G. D. Yadav, *Catal. Today*, 2018, **309**, 119-125.
24. G. Q. Lv, S. W. Chen, H. F. Zhu, M. Li and Y. X. Yang, *App. Surf. Sci.*, 2018, **458**, 24-31.
25. F. Nocito, M. Ventura, M. Aresta and A. Dibenedetto, *ACS Omega*, 2018, **3**, 18724-18729.
26. S. Xu, P. Zhou, Z. H. Zhang, C. J. Yang, B. G. Zhang, K. J. Deng, S. Bottle and H. Y. Zhu, *J. Am. Chem. Soc.*, 2017, **139**, 14775-14782.
27. Z. Z. Yang, W. Qi, R. X. Su and Z. M. He, *Energ. Fuel.*, 2016, **31**, 533-541.
28. D. K. Mishra, H. J. Lee, J. Kim, H. S. Lee, J. K. Cho, Y. W. Suh, Y. Yi and Y. J. Kim, *Green Chem.*, 2017, **19**, 1619-1623.
29. K. Gupta, R. K. Rai, A. D. Dwivedi and S. K. Singh, *ChemCatChem*, 2017, **9**, 2760-2767.
30. X. B. Zuo, A. S. Chaudhari, K. Snavely, F. H. Niu, H. Zhu and K. J. Martin, *AIChE J.*, 2017, **63**, 162-171.
31. W. Hou, Q. Wang, Z. J. Guo, J. Li, Y. Zhou and J. Wang, *Catal. Sci. Technol.*, 2017, **7**, 1006-1016.
32. M. Cui, R. L. Huang, W. Qi, R. X. Su and Z. M. He, *RSC Adv.*, 2017, **7**, 7560-7566.
33. E. Hayashi, T. Komanoya, K. Kamata and M. Hara, *ChemSusChem*, 2017, **10**, 654-658.
34. P. V. Rathod, S. D. Nale and V. H. Jadhav, *ACS Sustain. Chem. Eng.*, 2016, **5**, 701-707.
35. J. Zhao, J. Anjali, Y. B. Yan and J. M. Lee, *ChemCatChem*, 2017, **9**, 1187-1191.
36. F. Wang, L. Jiang, J. M. Wang and Z. H. Zhang, *Energ. Fuel.*, 2016, **30**, 5885-5892.
37. G. S. Yi, S. P. Teong and Y. G. Zhang, *Green Chem.*, 2016, **18**, 979-983.
38. Z. Y. Gui and W. Cao, *ChemCatChem*, 2016, **8**, 3636-3643.
39. Y. B. Wang, K. Yu, D. Lei, W. Si, Y. J. Feng, L. L. Lou and S. X. Liu, *ACS Sustain. Chem. Eng.*, 2016, **4**, 4752-4761.
40. Y. W. Zhang, Z. M. Xue, J. F. Wang, X. H. Zhao, Y. H. Deng, W. C. Zhao and T. C. Mu, *RSC Adv.*, 2016, **6**, 51229-51237.
41. X. W. Han, L. Geng, Y. Guo, R. Jia, X. H. Liu, Y. G. Zhang and Y. Q. Wang, *Green Chem.*, 2016, **18**, 1597-1604.
42. R. Q. Fang, R. Luque and Y. W. Li, *Green Chem.*, 2016, **18**, 3152-3157.

43. X. B. Zuo, P. Venkitasubramanian, D. H. Busch and B. Subramaniam, *ACS Sustain. Chem. Eng.*, 2016, **4**, 3659-3668.
44. D. Baruah, F. L. Hussain, M. Suri, U. P. Saikia, P. Sengupta, D. K. Dutta and D. Konwar, *Catal. Commun.*, 2016, **77**, 9-12.
45. C. Lucarelli, S. Galli, A. Maspero, A. Cimino, C. Bandinelli, A. Lolli, J. Velasquez Ochoa, A. Vaccari, F. Cavani and S. Albonetti, *J. Phys. Chem. C*, 2016, **120**, 15310-15321.
46. L. F. Liao, Y. Liu, Z. Y. Li, J. P. Zhuang, Y. B. Zhou and S. Chen, *RSC Adv.*, 2016, **6**, 94976-94988.
47. X. K. Li and Y. G. Zhang, *Green Chem.*, 2016, **18**, 643-647.
48. G. Q. Lv, H. L. Wang, Y. X. Yang, X. Li, T. S. Deng, C. M. Chen, Y. L. Zhu and X. L. Hou, *Catal. Sci. Technol.*, 2016, **6**, 2377-2386.
49. C. V. Nguyen, Y. T. Liao, T. C. Kang, J. E. Chen, T. Yoshikawa, Y. Nakasaka, T. Masuda and K. C. W. Wu, *Green Chem.*, 2016, **18**, 5957-5961.
50. G. Q. Lv, H. L. Wang, Y. X. Yang, T. S. Deng, C. M. Chen, Y. L. Zhu and X. Hou, *Green Chem.*, 2016, **18**, 2302-2307.
51. S. Li, K. M. Su, Z. H. Li and B. W. Cheng, *Green Chem.*, 2016, **18**, 2122-2128.
52. J. Artz, S. Mallmann and R. Palkovits, *ChemSusChem*, 2015, **8**, 672-679.
53. J. Artz and R. Palkovits, *ChemSusChem*, 2015, **8**, 3832-3838.
54. N. Mei, B. Liu, J. D. Zheng, K. L. Lv, D. G. Tang and Z. H. Zhang, *Catal. Sci. Technol.*, 2015, **5**, 3194-3202.
55. H. Ait Rass, N. Essayem and M. Besson, *ChemSusChem*, 2015, **8**, 1206-1217.
56. C. M. Zhou, W. P. Deng, X. Y. Wan, Q. H. Zhang, Y. H. Yang and Y. Wang, *ChemCatChem*, 2015, **7**, 2853-2863.
57. F. H. Xu and Z. H. Zhang, *ChemCatChem*, 2015, **7**, 1470-1477.
58. Y. Y. Guo and J. Z. Chen, *ChemPlusChem*, 2015, **80**, 1760-1768.
59. S. G. Wang, Z. H. Zhang and B. Liu, *ACS Sustain. Chem. Engin.*, 2015, **3**, 406-412.
60. G. Q. Lv, H. L. Wang, Y. X. Yang, T. S. Deng, C. M. Chen, Y. L. Zhu and X. L. Hou, *ACS Catal.*, 2015, **5**, 5636-5646.
61. S. M. McKenna, S. Leimkühler, S. Herter, N. J. Turner and A. J. Carnell, *Green Chem.*, 2015, **17**, 3271-3275.
62. R. L. Liu, J. Z. Chen, L. M. Chen, Y. Y. Guo and J. W. Zhong, *ChemPlusChem*, 2014, **79**, 1448-1454.

63. X. Wan, C. Zhou, J. Chen, W. Deng, Q. Zhang, Y. Yang and Y. Wang, *ACS Catal.*, 2014, **4**, 2175-2185.
64. G. D. Yadav and R. V. Sharma, *Appl. Catal., B: Environ.*, 2014, **147**, 293-301.
65. B. Saha, D. Gupta, M. M. Abu-Omar, A. Modak and A. Bhaumik, *J. Catal.*, 2013, **299**, 316-320.
66. Z. Z. Yang, J. Deng, T. Pan, Q. X. Guo and Y. Fu, *Green Chem.*, 2012, **14**, 2986-2989.
67. N. K. Gupta, S. Nishimura, A. Takagaki and K. Ebitani, *Green Chem.*, 2011, **13**, 824-827.
68. B. Liu, Z. H. Zhang, K. L. Lv, K. J. Deng and H. M. Duan, *Appl Catal A*, 2014, **472**, 64-71.
69. Y. M. Wang, B. Liu, K. C. Huang and Z. H. Zhang, *Ind Eng Chem Res.*, 2014, **53**, 1313-1319.
70. Z. H. Zhang, Z. L. Yuan, D. G. Tang, Y. S. Ren, K. L. Lv and B. Liu, *ChemSusChem*, 2014, **7**, 3496-3504.